

Collapse of an antibubble

Jun Zou,* Chen Ji, BaoGang Yuan, XiaoDong Ruan, and Xin Fu

State Key Laboratory of Fluid Power Transmission and Control, Zhejiang University, Hangzhou, China

(Received 8 March 2013; published 10 June 2013)

In contrast to a soap bubble, an antibubble is a liquid globule surrounded by a thin film of air. The collapse behavior of an antibubble is studied using a high-speed video camera. It is found that the retraction velocity of the thin air film of antibubbles depends on the thickness of the air film, e , the surface tension coefficient σ , etc., and varies linearly with $(\sigma/\rho e)^{1/2}$, according to theoretical analysis and experimental observations. During the collapse of the antibubble, many tiny bubbles can be formed at the rim of the air film due to the Rayleigh instability. In most cases, a larger bubble will emerge finally, which holds most of the volume of the air film.

DOI: 10.1103/PhysRevE.87.061002

PACS number(s): 47.55.df

I. INTRODUCTION

Antibubbles, a less common physical phenomenon than bubbles, were first reported in 1932 by Hughes and Hughes [1]. In contrast to a soap bubble, an antibubble is a liquid globule surrounded by a thin film of air. The physics of soap bubbles is well established [2], whereas very few studies have been conducted on antibubbles. The structure of the antibubble is able to separate two different kinds of liquid, implying a potential use in drug delivery and lubrication. With two liquid-gas interface, antibubbles provide twice the surface area of bubbles, which is in favor of chemical reactions or molecular interactions. These potential applications of antibubbles have attracted the interest of scientists worldwide [3–6].

Antibubbles can be easily generated by gently ejecting a drop or liquid column of surfactant solution into the same surfactant liquid, but it is difficult to keep them stable in the liquid for a long time because of the drainage air driven by the hydrostatic pressure gradient [7]. The stabilization of antibubbles has been investigated in recent years, and indicates that the duration depends on the fluid viscosity and the added surfactant, as well as surface contamination [8,9]. With a high-speed video camera, Dorbolo *et al.* [10] were the first to observe the whole process of the collapse of an antibubble, describing it as a “spectacular.” However, it is still unknown what affects the collapse velocity of antibubbles.

This paper attempts to reveal what influences the collapse velocity of antibubbles by using a high-speed video camera. A model of the collapse velocity of antibubbles is developed on the basis of the experimental observations.

II. EXPERIMENTAL SETUP

The schematic representation of the experimental setup is shown in Fig. 1, and is similar to a device for generating drops [11]. The antibubbles are generated by a syringe pump which was programmed to dispense the liquid at rates of 0–10 ml/s. In order to capture the details of the collapse, a high-speed video camera (FASTCAM-ultima APX, San Diego, CA) fitted with a Nikkor 60-mm microlens is used. Backlight is produced by a high-intensity light-emitting diode (LED) lamp with a thin sheet of drafting paper which is

used as a diffuser. Images are captured at a speed of 12 500 frames per second (fps). The radius of the antibubbles is measured by an image analyzer. The antibubble radius is $R_a = (D_x + D_y)/4$, where D_x is the horizontal diameter and D_y is the vertical diameter. A rectangular Plexiglass container ($8 \times 8 \times 100$ cm³) is used to hold a mixture of high-purity water and dishwashing soap. The liquid mixture and laboratory temperature are maintained at 25 °C. The uncertainties in the experiments are estimated. The size of the antibubble (D_x and D_y) is ± 0.02 mm, and the temperature is about ± 2 °C. The thickness of the air film, e , can be estimated by summing the volume of the bubbles produced during the collapse of the antibubbles,

$$e = \frac{\sum V_b}{4\pi R_a^2}, \quad (1)$$

where $\sum V_b$ represents the total volume of the bubbles produced by the collapse, which is measured by the image analyzer. R_a is the antibubble radius.

III. RESULTS AND DISCUSSION

According to our observation, the antibubbles do not always pop at the bottom at the beginning. In order to investigate the collapse of antibubbles more clearly, we punctured the air film with a pin. Figure 2 shows the collapse sequence of an antibubble. Once the air film is punctured with a pin, the inner liquid globule of the antibubble suddenly coalesces with the surrounding liquid. Then the air film begins to retract from the pierced point at a high speed. Finally, the air film shrinks into air bubbles. During the process, air ligaments emerging from the rim will ultimately break into tiny bubbles, like droplets from a bursting bubble [12], by capillary instability. Usually a larger bubble is generated after the collapse, which holds most of the volume of the air film in most cases, as shown in Fig. 3.

The ruptures of soap bubbles and antibubbles have something in common. Above all, the thicknesses of liquid film and air film are both up to micrometer order. The surface tension plays an important role in the collapse process. Crucial work has been done on the rupture of a thin spherical liquid film. For an inviscid liquid, a uniform film retracts at a constant speed $U = (2\sigma_l/h_l\rho_l)^{1/2}$ [13,14], where σ_l and ρ_l are the liquid surface tension and density, respectively, and h_l is the thickness of the liquid film. Considering the viscosity, the retracting film edge also eventually attains the same speed as in the inviscid

*junzou@zju.edu.cn

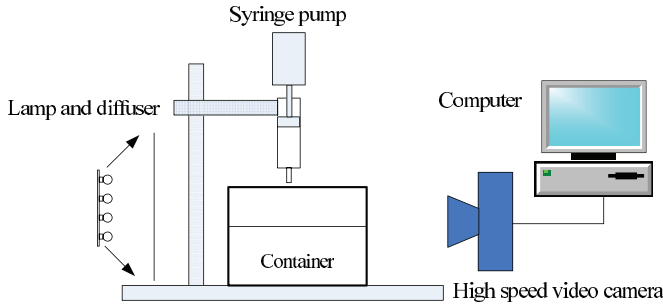


FIG. 1. (Color online) Experimental setup.

case, while the transient approach to the final speed depends on the Ohnesorge number [15].

The influential factors during antibubble collapse can be derived from the viewpoint of energy for the bursting of an air film which may be flat, spherical, or other shapes. The liquid around the air film is driven by the collapse process, forming a velocity field. Considering the collapse of a flat air film as shown in Fig. 4, the total kinetic energy of the liquid is

$$E_M = \left(\rho \int_{V_f} v^2 \right) / 2, \quad (2)$$

where E_M denotes the total kinetic energy of the fluid, and V_f is the entire volume of the fluid involved in the retraction process. In order to calculate E_M , we suppose that all the air of the vanished film is collected by an expanding rim, whose cross section is circular with a radius of a , as shown in Fig. 4.

The flow field around the air rim is axisymmetric, where the radius of the vanished area of the air film is denoted as R . Because $(R/a) \gg 1$, the effect of the air rim is considered to be negligible on the other side of the symmetry axis. Therefore,

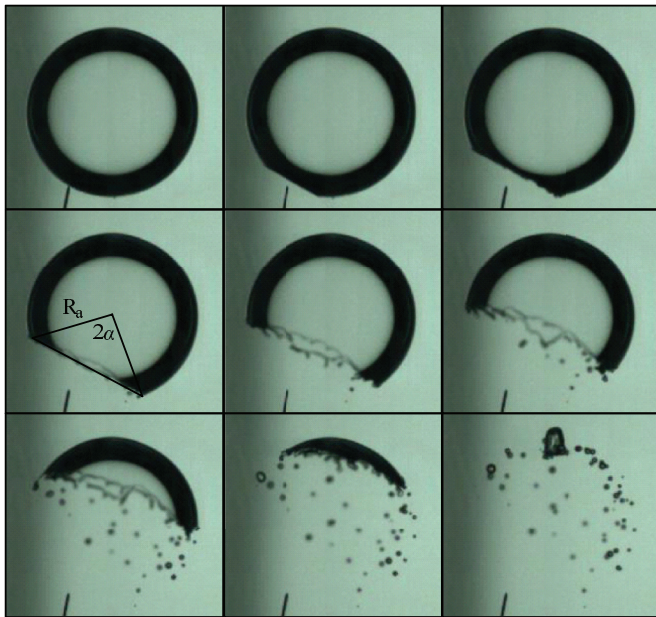


FIG. 2. (Color online) Collapse sequence of an antibubble ($R_a = 3.80$ mm) shown at intervals of 0, 0.8, 1.6, 2.4, 3.2, 4.0, 5.6, 7.2, and 11.2 ms (from left to right, from top to bottom). $\rho = 992$ kg/m³, $\sigma = 0.033$ N/m, $e = 2.95$ μ m, and the dark circumference of the antibubble is due to the total reflection on the fluid-air interface.

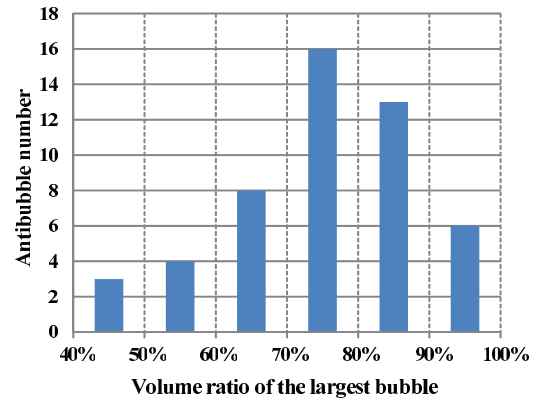


FIG. 3. (Color online) Statistic of the estimated volume ratio of the largest bubble to total bubbles produced during antibubble collapse. $\rho = 992$ – 999 kg/m³, $\sigma = 0.033$ – 0.055 N/m, $\mu = 1 \times 10^{-3}$ – 1.8×10^{-3} Pa s.

the flow field is approximately considered as potential flow around a cylinder with a constant translational speed of v_{rim} , where the velocity is calculated as

$$v_r = v_{rim}(a^2/r^2) \cos \theta, \quad v_\theta = v_{rim}(a^2/r^2) \sin \theta, \quad (3)$$

where v_{rim} denotes the retracting velocity of the rim, and (r, θ) are the polar coordinates, whose origin is located at the center of the air rim. The streamline of the flow field is shown in Fig. 4(b). E_M is then evaluated as

$$E_M \sim R \int_{\Omega} \left[\rho \left(\frac{v_{rim} a^2}{r^2} \right)^2 / 2 \right] d\Omega \sim \rho a^2 v_{rim}^2 R, \quad (4)$$

where Ω is the area of liquid on one side of the symmetry axis.

It is proved in the experiments that most air in the film usually ends up in the largest bubble, as shown in Fig. 3, so the air dissipation due to the unsteady rupture process is negligible. This volume balance gives

$$eR \sim a^2. \quad (5)$$

Combining (4) and (5), we find that

$$E_M \sim \rho e v_{rim}^2 R^2. \quad (6)$$

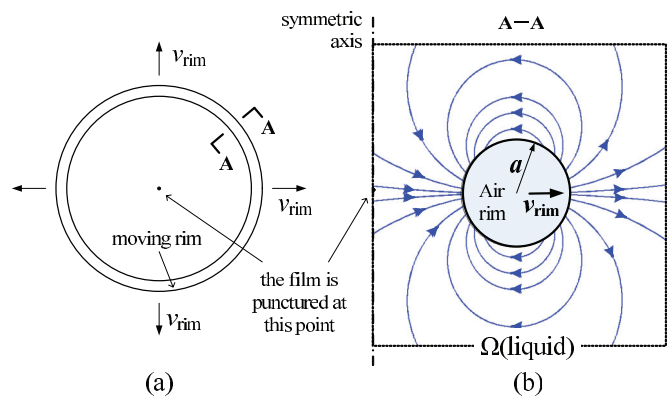


FIG. 4. (Color online) Diagram of planar air film bursting. (a) Top view; (b) section view of flow field around the rim of the air film.

In the case of liquid film collapse, the total kinetic energy has been proved to be proportional to the released surface energy [14,16]. For an antibubble, all the kinetic energy of the liquid also comes from the surface energy, as in the case of a liquid film. Therefore, the time derivation of the kinetic energy can be evaluated as

$$\sigma dA/dt \sim dE_M/dt \quad (7)$$

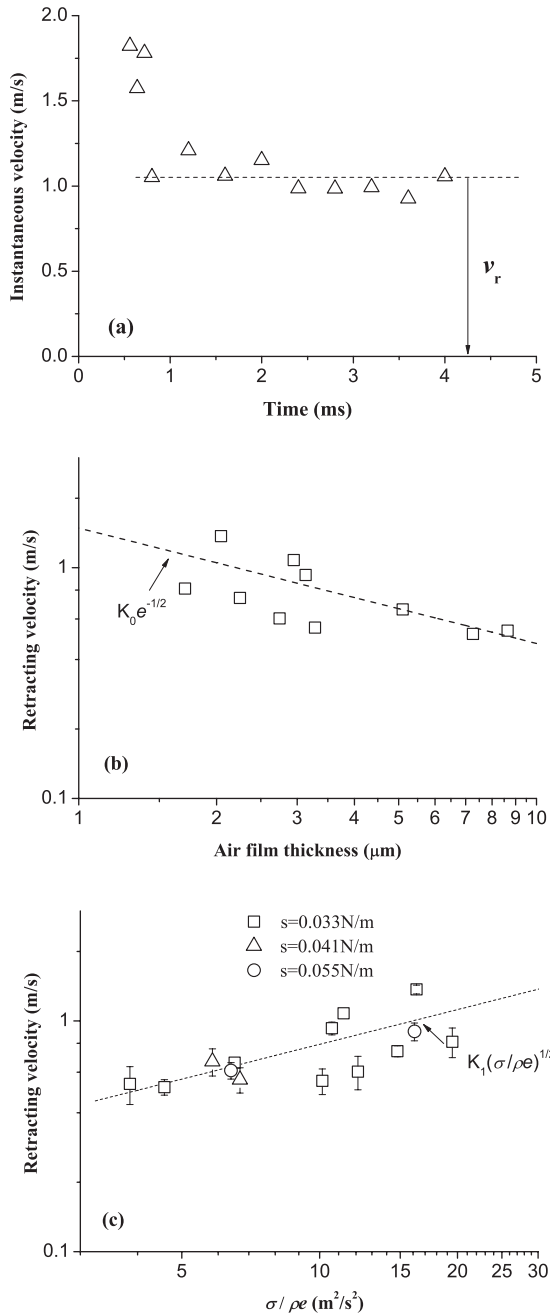


FIG. 5. Air film velocity of antibubbles, $K_0 = 1.48 \times 10^{-3} \text{ m}^{3/2}/\text{s}$, $K_1 = 0.235$. (a) The instantaneous velocity v_i of the air film during collapse ($R_a = 3.8 \text{ mm}$). (b) The retraction velocity v_{rim} with varying thickness of the air film over a range of $1.70\text{--}8.65 \mu\text{m}$ shown on a double logarithmic scale. (c) The retraction velocity v_{rim} for varying $(\sigma/\rho e)$ shown on a double logarithmic scale.

where A denotes the vanished area of the air film, $dA/dt = 2\pi R v_{rim}$. Combining (6) and (7), a solution to (7) is obtained as $dv_{rim}/dt = 0$, and $v_{rim} \sim (\sigma/\rho e)^{1/2}$.

Based on the experimental results, the instantaneous speed v_i of the air film of antibubbles can be calculated according to $v_i = R_a d\alpha/dt$, where α is the angle shown in Fig. 2. Figure 5(a) shows the instantaneous velocity v_i of the air film during antibubble collapse. After an initial quick increase, the instantaneous velocity of the air film decreases rapidly and approaches a constant, which is defined by us as the retracting velocity v_{rim} of air film. Due to the irregularity of the retracting rim, which is enhanced by the shedding of tiny bubbles, some data are missing.

Because the thickness of the air film of antibubbles is difficult to control quantitatively, we need to produce a lot of antibubbles to acquire a wide thickness distribution of air films to test our prediction. Moreover, in order to perform effective observations, the initial popping point of the antibubbles needs to be located on the focusing plane of a high-speed video camera. Representative data are shown in Fig. 5(b) for a mixed solution (volume fraction of dishwashing soap 7%, $\rho = 992 \text{ kg/m}^3$, $\sigma = 0.033 \text{ N/m}$, $\mu = 0.0018 \text{ Pa s}$). Each point corresponds to the measured thickness e and retracting velocity v_{rim} of the air film of a different antibubble. The data fall onto a single line and in Fig. 5(b), a power law $v_{rim} \sim (1/e)^{-1/2}$ is consistent with our data. Furthermore, we have changed the volume fraction of dishwashing soap of the mixture solution from 0.5% to 7% ($\rho = 992\text{--}999 \text{ kg/m}^3$, $\sigma = 0.033\text{--}0.055 \text{ N/m}$, $\mu = 1 \times 10^{-3}\text{--}1.8 \times 10^{-3} \text{ Pa s}$). Figure 5(c) shows the relation of the retraction velocity v_r of the air film with $\sigma/\rho e$; we can see that v_{rim} is well fitted by $(\sigma/\rho e)^{1/2}$, which validates the theoretical prediction very well. Therefore, a universal expression of the retraction velocity could be $v_{rim} = K_1 (\sigma/\rho e)^{1/2}$. By fitting the experimental data, the coefficient K_1 is evaluated to be 0.235 in the present study.

In the initial investigation of antibubble collapse, a number of interesting and important aspects of this problem have been neglected, among which are the influence of viscosity and surfactants, and non-Newtonian effects. In addition, we have considered only a uniform thickness of air film around the antibubble. The subsequent vortex evolution after antibubble collapse, as well as the Rayleigh capillary instability of the thin air film, remain as open problems. The latter effect can be clearly observed in Fig. 2.

IV. CONCLUSIONS

We have investigated the influence of the thickness of the air film and surface tension coefficient on the retraction velocity of air films based on experimental observations. The theoretical analysis and experimental results show that the retraction velocity of the air film varies linearly with $(\sigma/\rho e)^{1/2}$. During the collapse process of an antibubble, the instability of the air film causes the formation of many tiny bubbles. In most cases, a larger bubble finally emerges.

ACKNOWLEDGMENTS

This work is supported by the National Natural Science Foundation for Excellent Youth Scholars of China (Grant No.

51222501), the Science Fund for Creative Research Groups of the National Natural Science Foundation of China (Grant No.

51221004), and the National Natural Science Foundation of China (Grant No. 51075361).

-
- [1] W. Hughes and A. R. Hughes, *Nature (London)* **129**, 59 (1932).
 - [2] C. Isenberg, *The Science of Soap Films and Soap Bubbles* (Dover Publications, New York, 1992).
 - [3] A. M. Ganan-Calvo and J. M. Gordillo, *Phys. Rev. Lett.* **87**, 274501 (2001).
 - [4] A. Tufaile and J. C. Sartorelli, *Phys. Rev. E* **66**, 056204 (2002).
 - [5] M. Postema, F. J. Cate, G. Schmitz, N. Jong, and A. Wamel, *Lett. Drug Des. Discov.* **4**, 74 (2007).
 - [6] P. G. Kim and H. A. Stone, *Europhys. Lett.* **83**, 54001 (2008).
 - [7] S. Dorbolo, N. Vandewalle, E. Reyssat, and D. Quere, *Europhys. News* **37**, 24 (2006).
 - [8] P. G. Kim and J. Vogel, *Colloids Surf., A* **289**, 237 (2006).
 - [9] S. Dorbolo, D. Terwagne, R. Delhalle, J. Dujardin, N. Huet, N. Vandewalle, and N. Denkov, *Colloids Surf., A* **365**, 43 (2010).
 - [10] S. Dorbolo, H. Caps, and N. Vandewalle, *New J. Phys.* **5**, 161 (2003).
 - [11] J. Zou, P. F. Wang, T. R. Zhang, X. Fu, and X. D. Ruan, *Phys. Fluids* **23**, 044101 (2011).
 - [12] H. Lhuissier and E. Villermaux, *Phys. Fluids* **21**, 091111 (2009).
 - [13] W. E. Ranz, *J. Appl. Phys.* **30**, 1950 (1959).
 - [14] F. Culick, *J. Appl. Phys.* **31**, 1128 (1960).
 - [15] N. Savva and J. W. M. Bush, *J. Fluid Mech.* **626**, 211 (2009).
 - [16] A. B. Pandit and J. F. Davidson, *J. Fluid Mech.* **212**, 11 (1990).